

A Theoretical Study on the Borane-Catalyzed Reductive Amination of Aniline and Benzaldehyde with Dihydrogen: The Origins of Chemoselectivity

Jiyang Zhao,^{*,§} Shaoxian Liu,[§] Shanshan Liu, Wenwen Ding, Sijia Liu, Yao Chen, and Pan Du^{*}Cite This: *J. Org. Chem.* 2022, 87, 1194–1207

Read Online

ACCESS |



Metrics & More

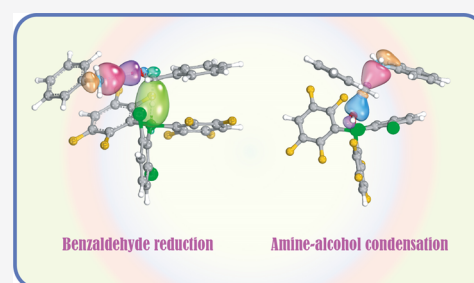


Article Recommendations



Supporting Information

ABSTRACT: Density functional theory calculations are used in this study to investigate the product selectivity and mechanism of borane-catalyzed reductive aldehyde amination by a H_2 reducing agent. Knowing that different boranes yield different products, two typical boranes, $B(2,6-Cl_2C_6H_3)(p-HC_6F_4)_2$ and $B-(C_6F_5)_3$, are studied. Of the seven possible pathways of $B(2,6-Cl_2C_6H_3)(p-HC_6F_4)_2$ -catalyzed aldehyde amination analyzed herein, four are favorable. Three of the four favorable pathways involve imine intermediates, and the fourth is a Lewis acid–base synergistic pathway that involves amine–alcohol condensation. As for the $B(C_6F_5)_3$ catalyst, it forms a highly stable Lewis adduct with aniline, which impedes the hydrogenation of imine. Therefore, the product of $B(C_6F_5)_3$ -catalyzed reductive amination of benzaldehyde and aniline is an imine. The linear relationship between the charge on the boron atom in the Lewis acid and the relative energies of the Lewis adduct and H_2 splitting transition state indicates that this parameter determines product selectivity. Indeed, when the natural charge on boron is larger than 1, an amine is produced, whereas when the charge is less than 1, an imine is produced. Hence, the selectivity of products can be controlled by adjusting the natural charge of the boron atom in the Lewis acid catalyst.



1. INTRODUCTION

Amines and alkylated amines are commonly occurring building blocks and essential precursors used in the construction of biologically active compounds, pharmaceuticals, agrochemicals, and industrial materials. As such, they have numerous applications in the fields of biology and chemistry.^{1,2} Although several methods have been proposed for the catalysis of amine functionalization reactions,² there is still a strong demand for the establishment of a green and sustainable reduction that can be used to synthesize multifunctional amines.³ Over the past decade, amazing progress has been achieved in the field of metal-free catalytic reductive amination particularly with the use of “frustrated Lewis pairs” (FLPs).⁴

The $B(C_6F_5)_3$ -catalyzed reductive amination of aldehydes and ketones was first reported by Ingleson in 2016, using hydrosilanes as reducing agents (Scheme 1a).⁵ The group of Zhong developed an asymmetric reductive system of ketone amination using $B(C_6F_5)_3$ as a catalyst and ammonia borane as a reductant (Scheme 1b).⁶ Recently, the groups of Soós and Ogoshi reported the borane-catalyzed reductive alkylation of amines with aldehydes using H_2 as the reducing agent (Scheme 1c).⁷

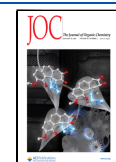
The commonly accepted mechanism of the reductive amination reaction consists of two steps: (I) aldehyde–amine condensation yielding an imine intermediate and (II) Lewis acid reduction yielding the amine product (Scheme 1d). For example, the mechanism of borane or borane/ H_2O -

catalyzed N-alkylation of amines with aldehydes involves the condensation of the two reactants (amine and aldehyde) to produce the imine (N-benzalaniline) intermediate followed by the reduction of this intermediate with hydrosilane.⁸

Considering that the chemical natures of H_2 and hydrosilane are different, it is expected that the mechanism of reductive ketone or aldehyde amination by H_2 is different from that of amination by hydrosilane. In this study, we investigate the mechanism underlying the Lewis acid $B(2,6-Cl_2C_6H_3)(p-HC_6F_4)_2$ -catalyzed reductive alkylation of aniline with benzaldehyde using H_2 as the reducing agent. Four possible reaction channels (Scheme 2) are proposed including (A) reaction initiation by H_2 splitting, followed by benzaldehyde reduction to primary alcohol and then $B(2,6-Cl_2C_6H_3)(p-HC_6F_4)_2$ -catalyzed aniline attack to give the amine product (Scheme 2A); (B) condensation of aniline and benzaldehyde, leading to the formation of an imine intermediate that is subsequently reduced to amine by $B(2,6-Cl_2C_6H_3)(p-HC_6F_4)_2$ and H_2 (Scheme 2B); (C) H_2 activation by $B(2,6-Cl_2C_6H_3)(p-HC_6F_4)_2$ and benzaldehyde, followed by the attack of aniline

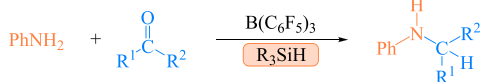
Received: October 19, 2021

Published: January 12, 2022

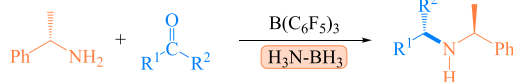


Scheme 1. Borane-Catalyzed Reductive Amination of Ketones or Aldehydes Using Different Reducing Agents ((a) Hydrosilane, (b) H_3NBH_3 , and (c) H_2); (d) Proposed Mechanism of the Reductive Amination of Ketones or Aldehydes with Amines

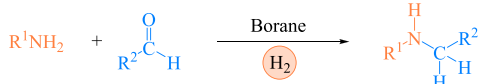
(a) $\text{B}(\text{C}_6\text{F}_5)_3$ -catalyzed reductive amination using hydrosilanes



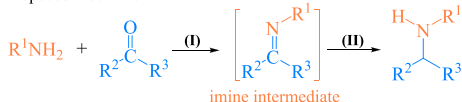
(b) $\text{B}(\text{C}_6\text{F}_5)_3$ -catalyzed asymmetric reductive amination with H_3NBH_3



(c) Borane-catalyzed reductive alkylation of amines using H_2



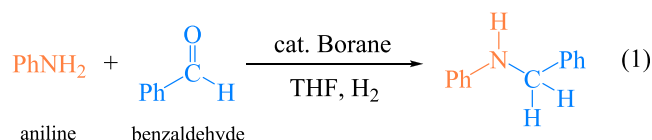
(d) Proposed mechanism



on the alcohol cation, yielding the amine product (Scheme 2C); (D) condensation of aniline and benzaldehyde followed by the reduction of the resulting imine intermediate under the

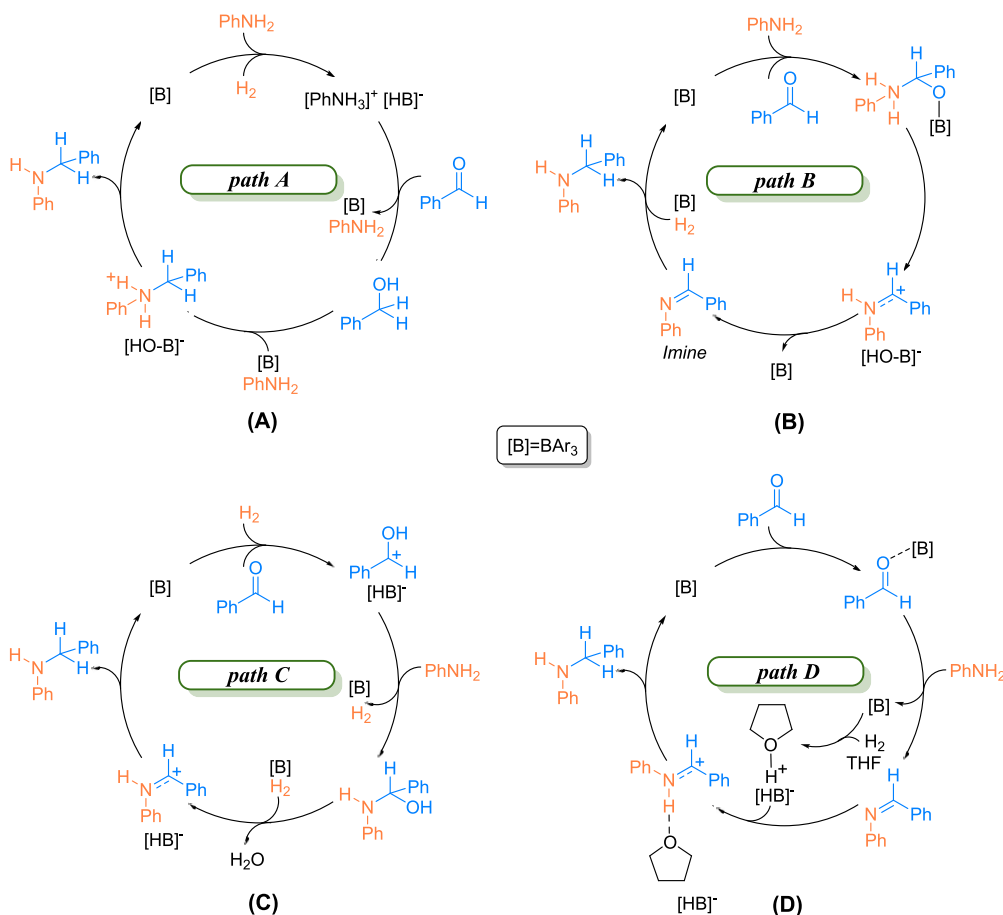
effect of the ion pair generated via FLP ($\text{B}(2,6\text{-Cl}_2\text{C}_6\text{H}_3)(\text{p-}\text{HC}_6\text{F}_4)_2$ and tetrahydrofuran (THF))-induced H_2 heterolysis (Scheme 2D).

The reaction channel D had been previously proposed by the group of Ogoshi, who considered that the THF solvent participates in the reaction by acting as a Lewis base.^{7a} Considering that the reaction can also take place in toluene solvent (i.e., in the absence of the THF Lewis base), with 45% product yield, it is anticipated that other reaction pathways, such as pathways A, B, or C, are also possible. Interestingly, the amine product changes when the borane catalyst is changed. The reason behind such a change remains unclear, which impedes the development and application of the amine alkylation reaction. Herein, density functional theory (DFT) calculations are used to analyze all possible molecular mechanisms of borane-catalyzed reductive amination of benzaldehyde with aniline in THF solvent using H_2 as the reducing agent (eq 1).



Borane: $\text{B}(2,6\text{-Cl}_2\text{C}_6\text{H}_3)(\text{p-}\text{FC}_6\text{F}_4)_2$, $\text{B}(\text{C}_6\text{F}_5)_3$

Scheme 2. Four Different Proposed Mechanisms of Ketone or Aldehyde Reductive Amination ((A) Amine-Alcohol Condensation Pathway, (B) Imine Pathway, (C) H_2 splitting by Borane and Benzaldehyde Pathway, (D) THF pathway)



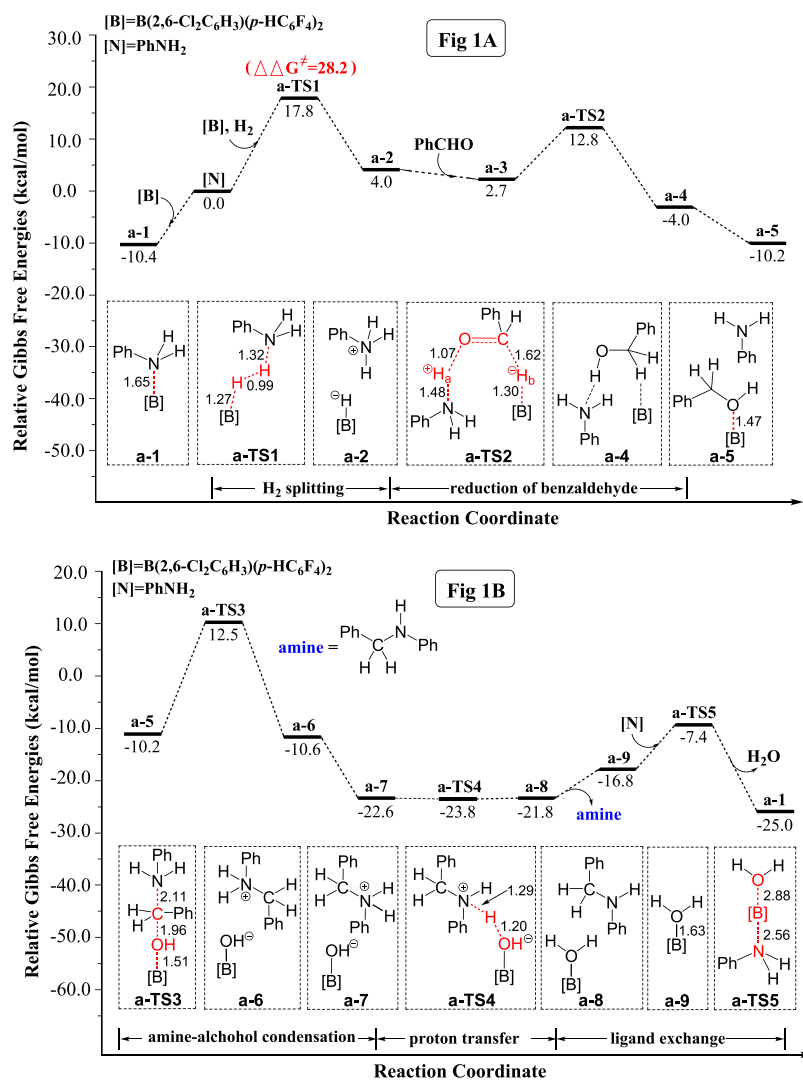


Figure 1. Free-energy profile of the reductive amination of benzaldehyde with aniline using H_2 as the reducing agent and $B(2,6\text{-Cl}_2\text{C}_6\text{H}_3)(p\text{-HC}_6\text{F}_4)_2$ catalyst (path A). Optimized structures of the stationary points (key bond lengths are given in Å).

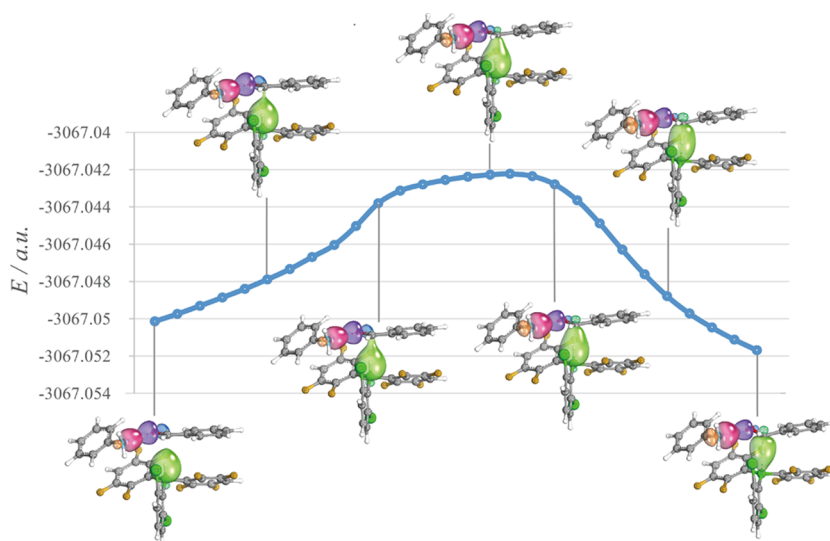


Figure 2. IBOs of the three reactive orbitals implicated in the reduction of benzaldehyde by a-2 via the a-TS2 transition state, along the reaction pathway.

2. RESULTS AND DISCUSSION

In this section, we discuss the four possible mechanisms of $B(2,6\text{-Cl}_2\text{C}_6\text{H}_3)(p\text{-HC}_6\text{F}_4)_2$ -catalyzed reductive aniline alkylation with benzaldehyde using H_2 . The chemoselectivities of this reaction and the $B(\text{C}_6\text{F}_5)_3$ -catalyzed reductive alkylation reaction are also analyzed. The optimized structures of all of the species in the following reaction pathways are shown in the Supporting Information (SI).

2.1. Mechanism of Pathway A (Lewis Acid–Base Synergistically Promoted Amine–Alcohol Condensation). First, we compare the possible Lewis adducts of $B(2,6\text{-Cl}_2\text{C}_6\text{H}_3)(p\text{-HC}_6\text{F}_4)_2$ with aniline, benzaldehyde, and THF. The results demonstrate that compared to benzaldehyde and THF, aniline exhibits better coordination with $B(2,6\text{-Cl}_2\text{C}_6\text{H}_3)(p\text{-HC}_6\text{F}_4)_2$, resulting in a more stable Lewis adduct (**a-1**). In fact, the free energy of **a-1** is $10.4 \text{ kcal mol}^{-1}$ lower than that of separated aniline and boron, which indicates that this adduct is the main existing form of the Lewis acid $B(2,6\text{-Cl}_2\text{C}_6\text{H}_3)(p\text{-HC}_6\text{F}_4)_2$ and is the reference point for the reaction. The optimized structures and relative free energies of the three Lewis adducts are illustrated in Figure S1 in the Supporting Information. In addition, as confirmed by the study of Guru et al.,^{3b} the Lewis adduct **a-1** is in equilibrium with free $B(2,6\text{-Cl}_2\text{C}_6\text{H}_3)(p\text{-HC}_6\text{F}_4)_2$ and aniline in the THF solvent.

The computed Gibbs free-energy profile of pathway A is presented in Figure 1A,B, and the optimized structures of intermediate and transition states along the pathway are shown in Figure S2 in the Supporting Information. As mentioned in the Introduction section, the catalytic cycle involves five key steps, including dihydrogen cleavage, aldehyde reduction, amine/alcohol condensation, proton migration, and catalyst regeneration. In the first reaction step, H_2 is split by the Lewis acid $B(2,6\text{-Cl}_2\text{C}_6\text{H}_3)(p\text{-HC}_6\text{F}_4)_2$ and aniline. The reaction proceeds via the **a-TS1** transition state and has a free-energy barrier of $28.2 \text{ kcal mol}^{-1}$ in THF (relative to **a-1**). This is a common FLP-promoted H_2 activation reaction that has been extensively studied by our group, as well as by other research groups.⁹ Notably, several structures of **a-TS1** were determined computationally, but only the most stable one is shown in Figure 2. The free-energy barriers of **a-TS1** calculated using B3LYP-*d3* and ω B97XD functionals are 24.6 and $25.3 \text{ kcal mol}^{-1}$, respectively. The product of the H_2 splitting reaction step is the H^+/H^- ion pair (**a-2**) that can be used for the hydrogenation of unsaturated compounds. We optimized the **a-2** ion pair using the 6-311++G(*d,p*) basis set including diffuse functions. The corresponding free energy is $3.1 \text{ kcal mol}^{-1}$ that is close to that calculated by the method defined in computational details ($4.0 \text{ kcal mol}^{-1}$).

The second step in the catalytic cycle is the reduction of benzaldehyde by **a-2** via the **a-TS2** transition state. This step has a free-energy barrier of $23.2 \text{ kcal mol}^{-1}$ in THF (relative to **a-1**). Based on the vibrational mode of **a-TS2**, H^+ and H^- are simultaneously transferred to benzaldehyde from the **a-2** ion pair. This can be demonstrated by the simultaneous formation of O-H_a and C-H_b bonds along the intrinsic reaction coordinate (IRC), as shown in Figure S3 in the Supporting Information. This result is different from that reported in other computational studies concerning the FLP (borane and solvent (e.g., THF))-catalyzed hydrogenation of carbonyl compounds. In these studies, the reaction of carbonyl hydrogenation occurs in a stepwise manner.¹⁰ Figure 2 shows that the intrinsic bond

orbitals (IBOs) transform continuously from the electronic structure of the starting material to that of the product, along the IRC. Three IBOs show a concerted transformation with one N-H σ bond transforming into a O-H σ bond and the B-H σ bond changing into a C-H σ bond. The reduction of benzaldehyde by **a-2** generates benzyl alcohol, a product that coordinates with $B(2,6\text{-Cl}_2\text{C}_6\text{H}_3)(p\text{-HC}_6\text{F}_4)_2$ to produce a classical Lewis adduct and a stable intermediate labeled **a-5**. Compared to free benzyl alcohol, the C-O bond in intermediate **a-5** is longer (1.47 vs 1.41 \AA), which indicates that this bond is activated by the strong electron-withdrawing effect of the Lewis acid $B(2,6\text{-Cl}_2\text{C}_6\text{H}_3)(p\text{-HC}_6\text{F}_4)_2$ in **a-5**. Such activation of the C-O bond facilitates subsequent nucleophilic attack by aniline.

In the third step of the alkylation reaction, the activated carbon in intermediate **a-5** undergoes nucleophilic attack by aniline, and the borane $B(2,6\text{-Cl}_2\text{C}_6\text{H}_3)(p\text{-HC}_6\text{F}_4)_2$ moiety abstracts the hydroxyl group from the benzyl alcohol moiety. The reaction occurs via the **a-TS3** transition state, and the corresponding free-energy barrier is $22.9 \text{ kcal mol}^{-1}$ in THF (relative to **a-1**). Under the combined action of $B(2,6\text{-Cl}_2\text{C}_6\text{H}_3)(p\text{-HC}_6\text{F}_4)_2$ and aniline, the amine and alcohol group undergo the condensation reaction. In this novel reaction mode of amine–alcohol condensation, the amine acts as both a reactant and Lewis base.¹¹ Two IBOs show a concerted transformation with one aniline lone pair (top) transforming into a C-N σ bond and the C-O σ bond (down) changing into a lone pair (Figure S4 in the Supporting Information). The product of such transformation is the ammonium intermediate **a-6**. Previously, Meng et al. had studied the $B(\text{C}_6\text{F}_5)_3$ -catalyzed alkylation of arylamines using benzylic alcohols.^{3c} Based on the reaction pathway they proposed, the borane–alcohol Lewis adduct dissociates to yield a carbocation, which in turn undergoes nucleophilic attack by the amine. Considering that the energy barrier of the pathway proposed by Meng et al. is higher than that of the pathway detailed herein (35.7 vs $28.2 \text{ kcal mol}^{-1}$), it is not likely that it would have a significant contribution under the investigated experimental conditions.

The **a-6** intermediate subsequently passes through a proton transfer transition state (**a-TS4**) to give the desired amine product (benzenamine) and the Lewis adduct $[\text{B}]\text{-H}_2\text{O}$ ($[\text{B}] = B(2,6\text{-Cl}_2\text{C}_6\text{H}_3)(p\text{-HC}_6\text{F}_4)_2$). The latter undergoes a bimolecular nucleophilic substitution reaction with aniline, and the reaction proceeds via the **a-TS5** ($\text{S}_{\text{N}}2@B$) transition state. Interestingly, the nucleophile (aniline) and leaving group (H_2O) implicated in the $\text{S}_{\text{N}}2$ reaction are both neutral,¹² and the free-energy barrier is only $15.2 \text{ kcal mol}^{-1}$ in THF (relative to **a-7**). The ligand exchange of aniline finally results in the regeneration of the **a-1** and free H_2O , thereby completing the catalytic reaction. In studies conducted by Fasano et al. and Chen et al.,^{5a,8} $[\text{B}]\text{-H}_2\text{O}$ acts as a Brønsted acid that catalyzes the *N*-alkylation reaction. However, there is a 4 \AA molecular sieve in our studied system, and the H_2O byproduct is absorbed by this sieve.

Overall, the results suggest that pathway A, that is, FLP-catalyzed aldehyde reduction by H_2 , followed by amine–alcohol condensation and ligand exchange, is energetically feasible, with an overall energy change of $-25.0 \text{ kcal mol}^{-1}$. The rate-limiting step is the splitting of H_2 by borane and aniline (via **a-TS1**), and it has a free-energy barrier of $28.2 \text{ kcal mol}^{-1}$. Pathway A does not involve an imine intermediate;

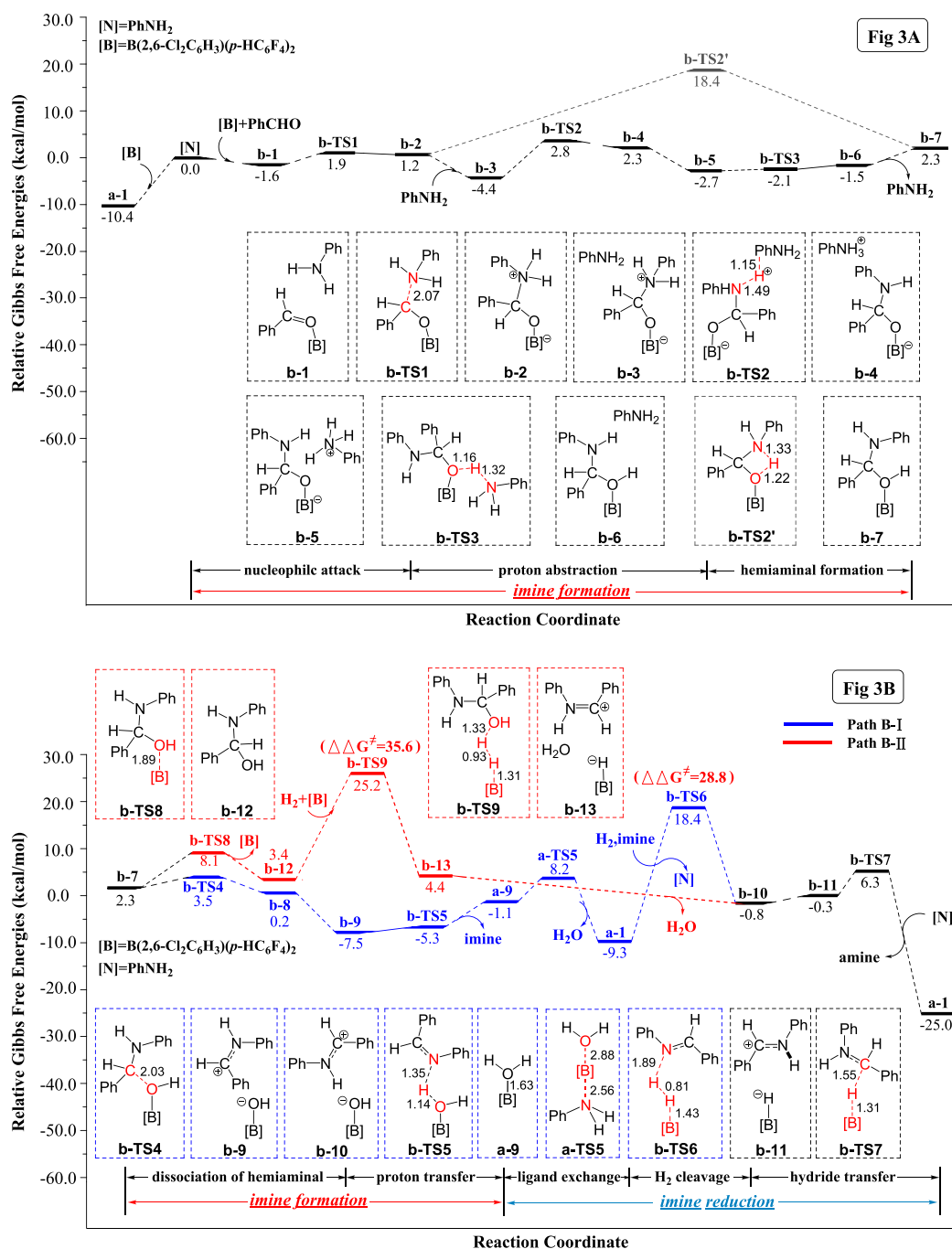


Figure 3. Free-energy profile of the Lewis acid $B(2,6-Cl_2C_6H_3)(p-HCF_4)_2$ -catalyzed reductive amination of aldehydes in which imine intermediate is generated to produce an amine via pathway B. Optimized structures of the stationary points (key bond lengths are given in Å).

however, it is possible under experimental conditions, as evidenced by the low free-energy barrier.

2.2. Mechanism of Pathway B (Imine Pathway). Based on our calculations, two main steps (imine formation and reduction) are implicated in pathway B, as shown in the free-energy profile illustrated in Figure 3. The optimized structures of all species along the pathway are shown in Figures S5 and S6 in the Supporting Information. In the first step, an imine intermediate is generated (Figure 3A and part of Figure 3B), and in the second step, this intermediate undergoes hydrogenation to form an amine (Figure 3B). The imine is formed via five successive elementary steps, namely, nucleophilic

attack, proton abstraction, hemiaminal formation, dissociation of hemiaminal, and proton transfer.

2.2.1. Imine Formation. First, borane $B(2,6-Cl_2C_6H_3)(p-HCF_4)_2$ and benzaldehyde coordinate to produce a Lewis adduct **b-1**. Then the nucleophilic attack of aniline on the carbonyl carbon occurs through transition state **b-TS1** as evidenced by the low free-energy barrier of the reaction ($12.3 \text{ kcal mol}^{-1}$ in THF, relative to **a-1**). Subsequently, a second aniline molecule assists in the migration of a proton from the ammonium moiety to the oxygen atom, resulting in the formation of a hemiaminal via transition states **b-TS2** ($13.2 \text{ kcal mol}^{-1}$) and **b-TS3** ($8.3 \text{ kcal mol}^{-1}$). The direct intramolecular proton transfer from ammonium to oxygen

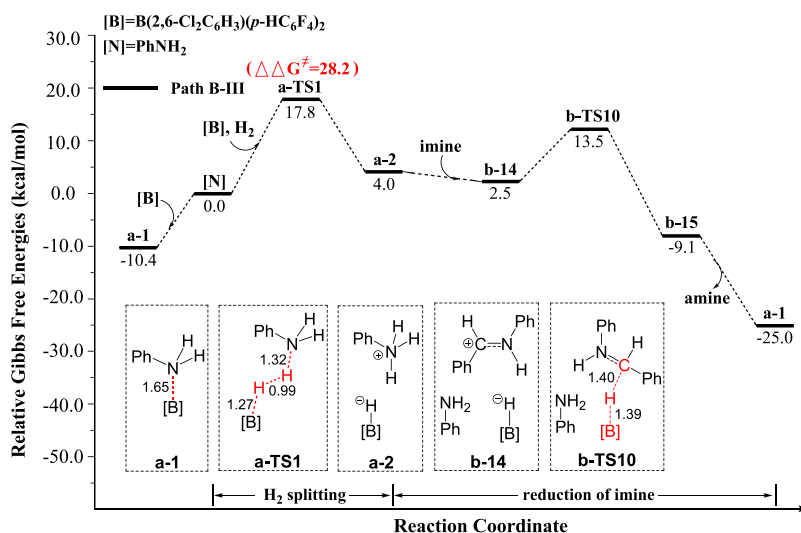


Figure 4. Free-energy profile of the FLP $\text{B}(\text{2,6-Cl}_2\text{C}_6\text{H}_3)(\text{p-HC}_6\text{F}_4)_2$ /aniline-catalyzed reductive amination of aniline and benzaldehyde by H_2 via the imine pathway (path B-III). Optimized structures of the stationary points (key bond lengths are given in Å).

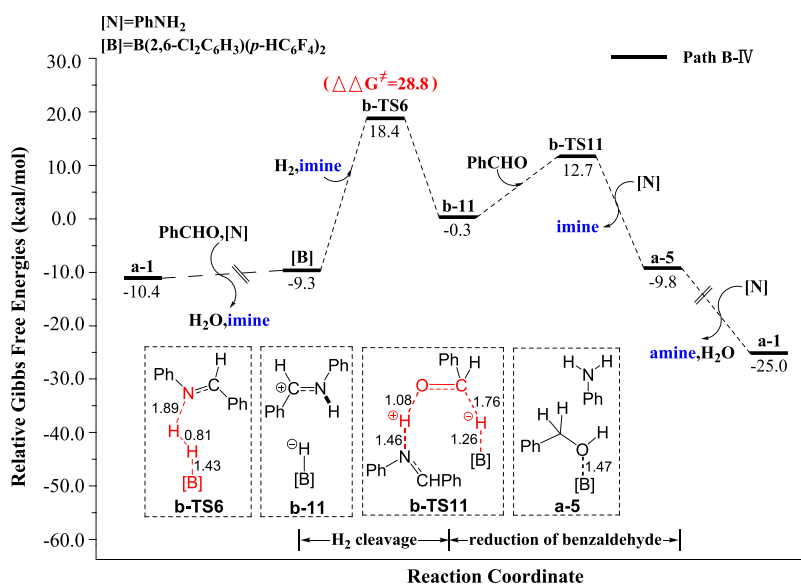


Figure 5. Free-energy profile of the FLP $\text{B}(\text{2,6-Cl}_2\text{C}_6\text{H}_3)(\text{p-HC}_6\text{F}_4)_2$ /imine-catalyzed reduction of benzaldehyde by H_2 via the imine pathway (path B-IV). Optimized structures of the stationary points (key bond lengths are given in Å).

via **b-TS2'** is also considered; however, this elementary step has a free-energy barrier of $28.8 \text{ kcal mol}^{-1}$, which is higher than that of the aniline-assisted pathway. The generated hemiaminal subsequently coordinates with borane $\text{B}(\text{2,6-Cl}_2\text{C}_6\text{H}_3)(\text{p-HC}_6\text{F}_4)_2$ to form a Lewis adduct **b-7**.

Two reaction pathways (B-I and B-II) are possible for the Lewis adduct **b-7**. Path B-I involves an imine intermediate, whereas path B-II does not. The iminium intermediate implicated in path B-I is generated upon the facile abstraction of a hydroxyl moiety from hemiaminal by the Lewis acid $\text{B}(\text{2,6-Cl}_2\text{C}_6\text{H}_3)(\text{p-HC}_6\text{F}_4)_2$ via transition state **b-TS4**. The free energy of this transition state is only $13.9 \text{ kcal mol}^{-1}$ higher than that of **a-1** in THF. The OH-abstraction reaction generates a cation; however, the energy required for this process is less than that reported by Meng et al.^{3c} The discrepancy is mainly attributed to the stabilizing effect of the lone pair of electrons on the nitrogen atom in iminium. In the next step, the imine product (*N*-benzalaniline) is generated by

intramolecular proton transfer from the iminium moiety to the anionic hydroxyboron moiety via transition state **b-TS5**. The free energy of this transition state is only $4.3 \text{ kcal mol}^{-1}$ higher than **a-1** in THF. Considering that the free-energy barrier of imine formation from aniline and benzaldehyde is only $13.9 \text{ kcal mol}^{-1}$ and that of the reverse process is only $11.0 \text{ kcal mol}^{-1}$, the reaction is reversible. Moreover, the low reaction barrier associated with this reaction is consistent with the previously reported experimental result of 83% imine yield obtained within 5 min.^{7a}

2.2.2. Imine Reduction. Imine hydrogenation is an extensively studied reaction that involves dihydrogen cleavage and hydride transfer.¹³ In this study, the presence of the H_2O byproduct implies that an additional ligand exchange step (**a-TS5**, $18.6 \text{ kcal mol}^{-1}$ relative to **a-1**) is implicated in the reaction. The H_2 reducing agent is first split by imine (Lewis base) and borane $\text{B}(\text{2,6-Cl}_2\text{C}_6\text{H}_3)(\text{p-HC}_6\text{F}_4)_2$ via transition state **b-TS6**. The free-energy barrier of the splitting reaction is

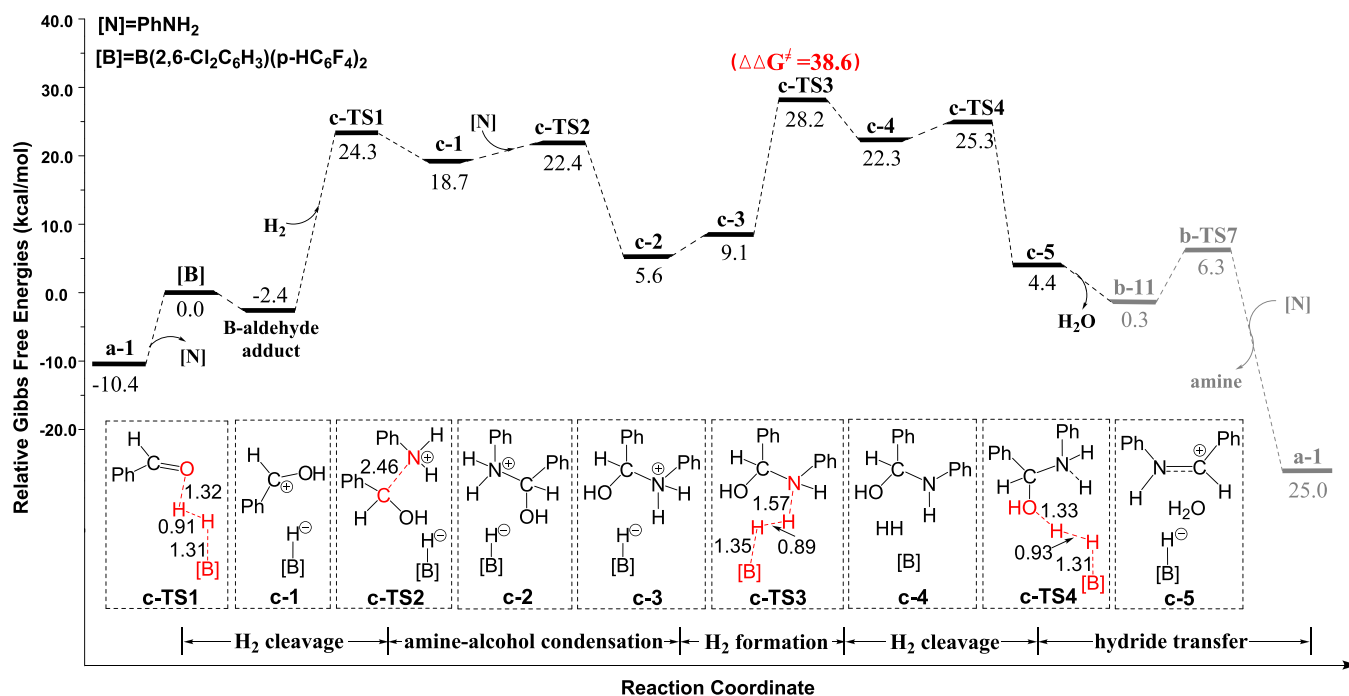


Figure 6. Free-energy profile of the FLP $(\text{B}(2,6\text{-Cl}_2\text{C}_6\text{H}_3)(p\text{-HC}_6\text{F}_4)_2)$ /benzaldehyde-catalyzed reductive amination of aniline and benzaldehyde by H_2 via pathway C. Optimized structures of the stationary points (key bond lengths are given in Å).

28.8 kcal mol⁻¹ in THF (relative to **a-1**), and this step is the rate-determining step along path B-I. To confirm the validity of the barrier, the **b-TS6** transition state was studied using B3LYP-*d3* and ω B97XD functionals, and the calculated free-energy barriers are 26.5 and 27.1 kcal mol⁻¹, respectively. Considering that all three methods used herein yield similar results, our calculated energy values are reasonable and valid. Finally, the transfer of hydride from hydridoborate to the iminium moiety leads to the desired product (benzenamine) via **b-TS7**. IBOs of the two reactive orbitals implicated in the reduction of imine via the **b-TS7** transition state along the reaction pathway are shown in Figure S7 in the Supporting Information.

In path B-II, **b-7** dissociates into free hemiaminal and borane $\text{B}(2,6\text{-Cl}_2\text{C}_6\text{H}_3)(p\text{-HC}_6\text{F}_4)_2$ via transition state **b-TS8** (18.5 kcal mol⁻¹ higher than **a-1** in free energy). Subsequently, H_2 is split by hemiaminal and borane $\text{B}(2,6\text{-Cl}_2\text{C}_6\text{H}_3)(p\text{-HC}_6\text{F}_4)_2$, which act as a Lewis acid and base, respectively. This leads to the formation of **b-14** ion pairs via transition state **b-TS9**. The free energy of this transition state lies at 35.6 kcal mol⁻¹ above **a-1** in THF. Considering that the energy barrier associated with **b-TS9** is higher than that corresponding to **b-TS6** (28.8 kcal mol⁻¹), path B-II is less energetically favorable than path B-I. Subsequently, the H_2O byproduct dissociates from **b-13**, and the **b-10** ion pair is formed. The next steps are the same as those implicated in path B-I.

The reduction of imine by ion pair **a-2** (path B-III) is also considered, and the corresponding free-energy profile is shown in Figure 4. First, the imine abstracts a proton from **a-2**, thereby generating an iminium intermediate **b-14**. Then, PhNH_2 is liberated from **b-14**, resulting in the formation of the **b-11** ion pair. The subsequent transfer of hydride via transition state **b-TS10** leads to the amine product, and the associated free-energy barrier is 23.9 kcal mol⁻¹. The rate-limiting step in path B-III is also the H_2 -splitting step (**a-TS1**), whose free-energy barrier is 28.2 kcal mol⁻¹.

In addition, the imine–borane complex also exists in equilibrium under the reaction conditions. We investigated the reduction of benzaldehyde by the **b-11** ion pair that was generated by the FLP $(\text{B}(2,6\text{-Cl}_2\text{C}_6\text{H}_3)(p\text{-HC}_6\text{F}_4)_2)$ /imine-induced H_2 splitting through the **b-TS6** transition state. The corresponding free-energy profile is shown in Figure 5 (path B-IV). The benzaldehyde is reduced by **b-11** ion pair via transition state **b-TS11** with a free-energy barrier of 23.1 kcal mol⁻¹. In **b-TS11**, H^+ and H^- are simultaneously transferred to benzaldehyde from the **b-11** ion pair based on the vibrational mode. After this step, the following reaction steps are the same as those implicated in path A (shown in Figure 1). The rate-determining step in path B-IV is also the cleavage of H_2 by borane $(\text{B}(2,6\text{-Cl}_2\text{C}_6\text{H}_3)(p\text{-HC}_6\text{F}_4)_2)$ and imine (**b-TS6**) with a free-energy barrier of 28.8 kcal mol⁻¹.

Overall, there are four possible pathways in mechanism B (paths B-I, B-II, B-III, and B-IV). With barriers of 28.8, 28.2, and 28.8 kcal mol⁻¹, respectively, paths B-I, B-III, and B-IV are more favorable than path B-II (barrier of 35.6 kcal mol⁻¹) and can occur under experimental conditions. Paths B-I, B-III, and B-IV involve an imine intermediate, which is consistent with the possible pathways proposed by the groups of Ogoshi and Wei.^{7a,8}

2.3. Mechanism of Pathway C (H_2 Splitting by the FLP Composed of Borane and Benzaldehyde). The free-energy profile of pathway C is shown in Figure 6, and the optimized structures of all species along the pathway are shown in Figure S8 in the Supporting Information. First, H_2 is split by Lewis acid $\text{B}(2,6\text{-Cl}_2\text{C}_6\text{H}_3)(p\text{-HC}_6\text{F}_4)_2$ and benzaldehyde via a reaction similar to that studied by Privalov, Soós, and Pati.¹⁰ The transition state **c-TS1** associated with this reaction lies at 34.7 kcal mol⁻¹ above **a-1** (free energy in THF). Based on this energy value, the barrier of the H_2 splitting reaction is higher than that reported in prior studies,¹⁰ probably because of the increased stability of the Lewis adduct **a-1**.

Following the splitting of H_2 , amine–alcohol condensation takes place via transition state **c-TS2**. The free-energy barrier of this transition state ($32.8 \text{ kcal mol}^{-1}$) is much higher than that of the similar **a-TS3** transition state in pathway A because of the lack of the carbocation stabilizing effect of Lewis acid $B(2,6\text{-Cl}_2\text{C}_6\text{H}_3)(p\text{-HC}_6\text{F}_4)_2$. The product of amine–alcohol condensation is a hemiaminal cation **c-2** that undergoes isomerization to give the **c-3** ion pair. The proximity between the adjacent hydridoborate and ammonium cation groups in **c-3** result in a weak $B\cdots H\cdots H\cdots N$ interaction, which leads to the generation of H_2 via transition state **c-TS3**. The free-energy barrier associated with this reaction is as high as $38.6 \text{ kcal mol}^{-1}$. Subsequently, the in situ-generated dihydrogen is split by Lewis acid $B(2,6\text{-Cl}_2\text{C}_6\text{H}_3)(p\text{-HC}_6\text{F}_4)_2$ and hemiaminal via **c-TS4**, resulting in the production of H_2O and ion pair **b-11**. The following steps in the mechanism are similar to those determined for pathway B.

Considering that the free-energy barrier of pathway C is $35.6 \text{ kcal mol}^{-1}$ (**c-TS3**), this mechanism is unfavorable.

2.4. Mechanism of Pathway D (H_2 Splitting by the FLP Composed of Borane and THF). Pathway D was first proposed by Hoshimoto et al., and it involves the splitting of H_2 to yield an ion pair followed by the subsequent reduction of imine.^{7a} The free-energy profile of this pathway is shown in Figure 7, and the optimized structures of all species along the

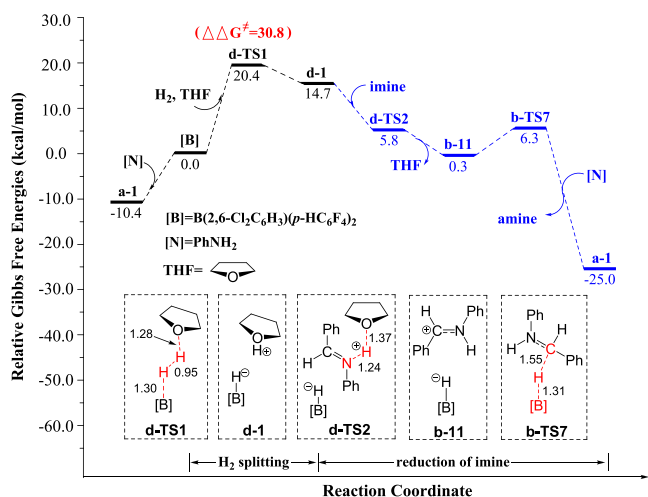


Figure 7. Free-energy profile of the FLP $B(2,6\text{-Cl}_2\text{C}_6\text{H}_3)(p\text{-HC}_6\text{F}_4)_2/\text{THF}$ -catalyzed reductive amination of aniline and benzaldehyde by dihydrogen (path D). Optimized structures of the stationary points (key bond lengths are given in Å).

pathway are shown in Figure S9. First, dihydrogen is split by the FLP composed of Lewis acid $B(2,6\text{-Cl}_2\text{C}_6\text{H}_3)(p\text{-HC}_6\text{F}_4)_2$ and THF (Lewis base) via transition state **d-TS1**. The resulting ion pair **d-1** bearing H^+ and H^- promotes the hydrogenation of imine. According to Heshmat and Privalov, the free-energy barrier of heterolytic H_2 cleavage by THF is

about 20 kcal mol^{-1} .^{10a} However, the barrier determined herein for H_2 splitting by $B(2,6\text{-Cl}_2\text{C}_6\text{H}_3)(p\text{-HC}_6\text{F}_4)_2$ and THF is as high as $30.8 \text{ kcal mol}^{-1}$ (**d-TS1**, see Figure 7). The difference is attributed to the increased stability of the **a-1** adduct formed in the latter case. The amine product is finally formed by imine reduction via transition states **d-TS2** (proton abstraction, $16.2 \text{ kcal mol}^{-1}$) and **b-TS7** (hydride transfer, $16.7 \text{ kcal mol}^{-1}$). Considering that the energy barrier of the rate-limiting H_2 splitting step in pathway D is high ($30.8 \text{ kcal mol}^{-1}$), THF cannot adequately mediate the reductive amination of aniline and benzaldehyde.

2.5. Discussion on the Favorable Mechanism. The results discussed in Sections 2.12.22.32.4 show that the free-energy barriers of pathways (A, B-I, B-II, B-III, B-IV, C, and D) implicated in the $B(2,6\text{-Cl}_2\text{C}_6\text{H}_3)(p\text{-HC}_6\text{F}_4)_2$ -catalyzed reductive amination of aniline and benzaldehyde by dihydrogen are 28.2, 28.8, 35.6, 28.2, 28.8, 38.6, and $30.8 \text{ kcal mol}^{-1}$, respectively (Table 1). Obviously, paths A, B-I, B-III, and B-IV are favorable, whereas paths B-II, C, and D are not. Based on B3LYP-d3 and ω B97XD calculations, paths A and B-III are slightly more likely to occur than paths B-I and B-IV under experimental conditions. The calculated reaction barriers are in good agreement with experimental data determined at 100°C ^{7a} or 80°C .^{7b} Heterolytic H_2 cleavage is the rate-limiting step in pathways A (**a-TS1**), B-I (**b-TS6**), B-III (**a-TS1**), and B-IV (**b-TS6**). In previous studies, it was found that the experimental product yield increases with increasing H_2 pressure, which confirms that H_2 splitting is the rate-limiting step.^{7a} Overall, our proposed paths A, B-I, B-III, and B-IV are in accordance with the experimental observations.

The differences observed in the H_2 splitting transition state corresponding to the seven proposed reaction pathways are attributed to variations in the Lewis bases. Table 2 compares the basicity and proton affinity of these bases, and the reported values suggest that aniline and imine are stronger bases and are more capable of splitting H_2 . Other Lewis bases, including hemiaminal, benzaldehyde, and THF, are less basic than aniline and are unable to split H_2 under experimental conditions. The strong Lewis bases used in paths A, B-I, B-III, and B-IV result in lower energy barriers compared to paths B-II, C, and D. Therefore, it may be concluded that the Lewis base determines which path is favorable.

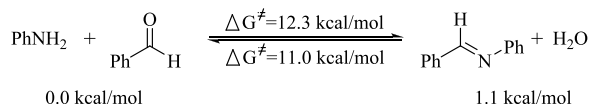
Imine intermediates are involved in paths B-I, B-III, and B-IV, which agrees well with previous experimental observations.^{7a} However, pathway A contradicts the experiments, as it does not involve an imine intermediate. To explain this contradiction, we must consider that the process of imine formation is reversible, as shown in Scheme 3. In experiments, about 10% of the benzaldehyde reactant was constantly observed throughout the reaction,^{7a} which confirms the equilibrium between the imine formation and hydrolysis under reaction conditions. Such equilibrium allows for the H_2 splitting by borane and aniline via path A. Recently, the groups of Maji, Zhao, and Chan separately developed a

Table 1. Free-Energy Barriers of the Rate-Limiting Steps in Different Proposed Pathways of $B(2,6\text{-Cl}_2\text{C}_6\text{H}_3)(p\text{-HC}_6\text{F}_4)_2$ -Catalyzed Reductive Amination of Aniline and Benzaldehyde with Dihydrogen (Unit: kcal mol^{-1})

	path A	path B-I	path B-II	path B-III	path B-IV	path C	path D
free-energy barrier (M062X)	28.2	28.8	35.6	28.2	28.8	38.6	30.8
free-energy barrier (B3LYP-d3)	24.6	26.5	/	24.6	26.5	/	/
free-energy barrier (ω B97XD)	25.3	27.1	/	25.3	27.1	/	/

Table 2. Proton Affinities of Five Lewis Bases and the Free-Energy Barriers of H₂ Splitting by B(2,6-Cl₂C₆H₃)(*p*-HC₆F₄)₂ and These Lewis Bases (Unit: kcal mol⁻¹)

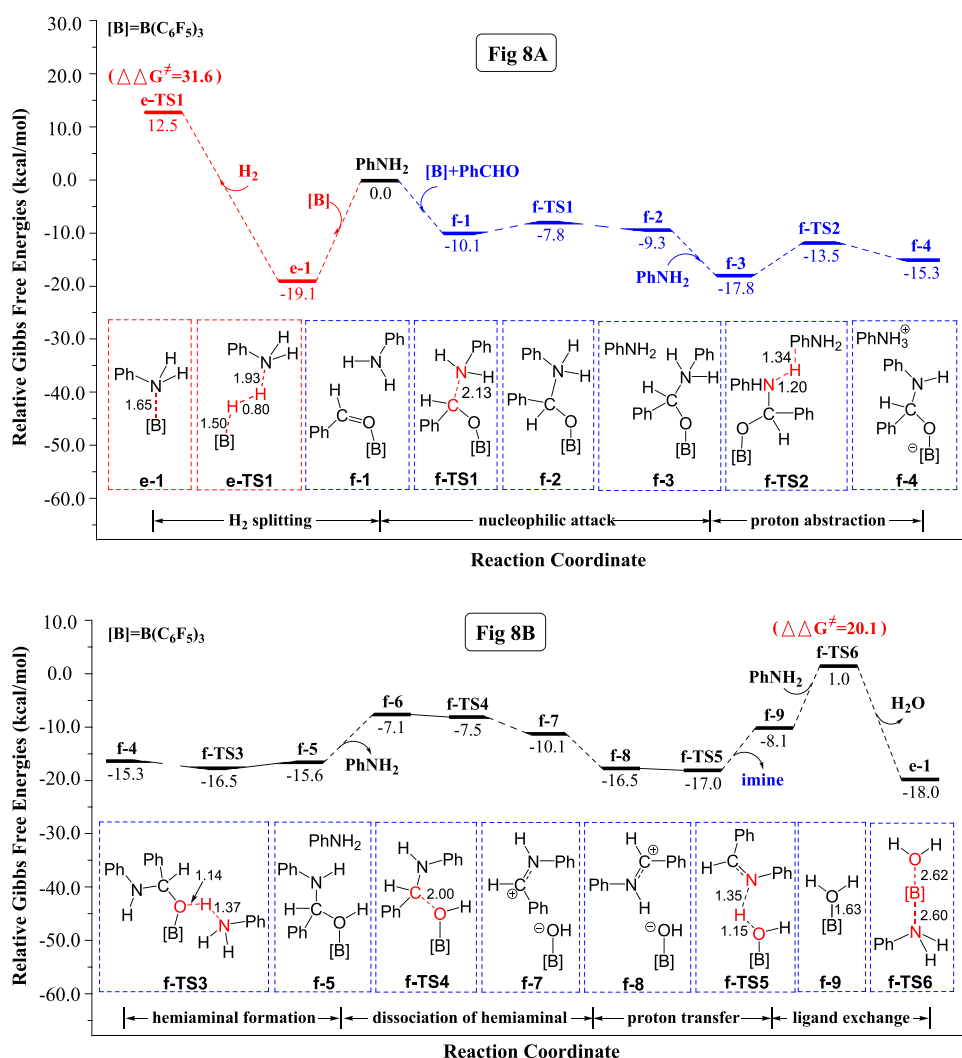
	path A	path B-I	path B-II	path B-III	path B-IV	path C	path D
Lewis base	aniline	imine	hemiaminal	aniline	imine	benzaldehyde	THF
TS	a-TS1	b-TS6	b-TS9	a-TS1	b-TS6	c-TS1	d-TS1
proton affinity	169.1	170.8	161.3	169.1	170.8	148.1	153.7
ΔG (TS)	28.2	28.8	35.6	28.2	28.8	38.6	30.8

Scheme 3. Equilibrium between the Formation and Hydrolysis of Imine under Reaction Conditions

promising borane B(C₆F₅)₃-catalyzed direct N-alkylation reaction of amine with benzylic alcohols,^{3b,c} which suggests that the amine–alcohol condensation mechanism along path A is feasible.

Overall, the results indicate that the B(2,6-Cl₂C₆H₃)(*p*-HC₆F₄)₂-catalyzed reductive amination of aniline and benzaldehyde by dihydrogen may proceed via four possible

pathways. Path A is initiated by the cleavage of H₂ under the effect of borane and aniline. The H₂-splitting step is followed by benzaldehyde hydrogenation to form benzylic alcohol and then amine–alcohol condensation to yield the amine product. The other three possible pathways involve imine intermediates. The generated imines undergo hydrogenation by two different ion pairs. In path B-I, the ion pair is formed upon H₂ splitting by Lewis acid B(2,6-Cl₂C₆H₃)(*p*-HC₆F₄)₂ and the imine itself. Meanwhile, in path B-III, the ion pair is generated upon the splitting of H₂ by Lewis acid B(2,6-Cl₂C₆H₃)(*p*-HC₆F₄)₂ and aniline. Path IV is similar to path A, except that H₂ is split by imine and Lewis acid B(2,6-Cl₂C₆H₃)(*p*-HC₆F₄)₂ in the first step. Paths B-I and B-III are similar with prior studies, but paths A and IV are novel mechanisms proposed for the B(2,6-

**Figure 8.** Free-energy profile of the B(C₆F₅)₃-catalyzed reductive amination of aniline and benzaldehyde by dihydrogen. Optimized structures of the stationary points (key bond lengths are given in Å).

$\text{Cl}_2\text{C}_6\text{H}_3$)($p\text{-HC}_6\text{F}_4$)₂-catalyzed reductive amination of aniline and benzaldehyde by dihydrogen.

2.6. Other Lewis Acids. According to previous experimental studies, the yield of the amine product produced in THF via the $\text{B}(2,6\text{-Cl}_2\text{C}_6\text{H}_3)$ ($p\text{-HC}_6\text{F}_4$)₂-catalyzed reductive amination of aniline and benzaldehyde is greater than 99%. The use of other triarylborane catalysts such as $\text{B}(\text{C}_6\text{F}_5)_3$, $\text{B}(\text{C}_6\text{Cl}_5)(\text{C}_6\text{F}_5)_2$, $\text{B}(p\text{-HC}_6\text{F}_4)_3$, and BPh_3 results in the generation of imines as the main product.^{7a} In this study, borane $\text{B}(\text{C}_6\text{F}_5)_3$ was chosen as another catalyst of reductive amination to explore how the Lewis acid determines the selectivity of products. The corresponding free-energy profile is shown in Figure 8A,B, and the optimized intermediates and transition states are shown in Figures S11 and S12 in the Supporting Information.

Two possible pathways of $\text{B}(\text{C}_6\text{F}_5)_3$ -catalyzed reductive amination of aniline and benzaldehyde are considered. The first pathway is similar to path A shown in Figure 1. This pathway (shown in Figure 8A) is initiated by H_2 splitting under the effect of the $\text{B}(\text{C}_6\text{F}_5)_3$ Lewis acid and aniline. The initiation step proceeds via the e-TS1 transition state characterized by a free-energy barrier of 31.6 kcal mol⁻¹ in THF (relative to e-1). Clearly, the barrier is large, which indicates that the generation of amine via this pathway is difficult under experimental conditions. The main reason behind such a high energy is that the Lewis adduct e-1 formed by $\text{B}(\text{C}_6\text{F}_5)_3$ and aniline is very stable (−19.1 kcal mol⁻¹, $\text{B}(\text{C}_6\text{F}_5)_3 + \text{aniline} \rightarrow \text{e-1}$). Considering that the acidity of $\text{B}(\text{C}_6\text{F}_5)_3$ (−71.7 kcal mol⁻¹) is greater than that of $\text{B}(2,6\text{-Cl}_2\text{C}_6\text{H}_3)$ ($p\text{-HC}_6\text{F}_4$)₂ (−62.8 kcal mol⁻¹), the Lewis adduct e-1 is more stable than a-1.

The other pathway (shown in Figure 8B) involves the generation of imine and is similar to pathway B-I shown in Figure 2. The process involves several steps including nucleophilic attack of aniline on benzaldehyde (f-TS1, 11.3 kcal mol⁻¹), proton migration (f-TS2, 5.6 kcal mol⁻¹), hydride transfer (f-TS3, 2.6 kcal mol⁻¹), C–O bond breaking (f-TS4, 11.6 kcal mol⁻¹), imine generation (f-TS5, 2.1 kcal mol⁻¹), and ligand exchange (f-TS6, 20.1 kcal mol⁻¹). The last step has the highest free-energy barrier and is thus the rate-limiting step. The reaction is facilitated by exothermicity (18.0 kcal mol⁻¹) and the generation of the H_2O byproduct that can be absorbed by a 4 Å molecular sieve. Overall, the results indicate that the formation of an imine intermediate by the $\text{B}(\text{C}_6\text{F}_5)_3$ -catalyzed reductive amination of aniline and benzaldehyde with H_2 can easily occur.

As shown in Figure 9, $\text{B}(\text{C}_6\text{F}_5)_3$ -catalyzed reduction of imine by H_2 proceeds via transition state f-TS7. However, considering that f-TS7 lies at 33.4 kcal mol⁻¹ above the Lewis adduct e-1, further reduction of the imine to yield the amine product is unlikely under experimental conditions. This is consistent with previous experimental reports showing that imines are the main products of the reductive aniline and benzaldehyde amination reaction catalyzed by $\text{B}(\text{C}_6\text{F}_5)_3$.

2.7. Selectivity of Products. As mentioned in the introduction, the product of reductive aniline and benzaldehyde amination by dihydrogen varies depending on the nature of the Lewis acid catalyst used. Table 3 summarizes the products obtained using catalysts B1 ($\text{B}(2,6\text{-Cl}_2\text{C}_6\text{H}_3)$ ($p\text{-HC}_6\text{F}_4$)₂),^{7a} B2 ($\text{B}(2\text{-Cl-5-FC}_6\text{H}_3)_3$),^{7b} B3 ($\text{B}(2,6\text{-Cl}_2\text{C}_6\text{H}_3)_2(2\text{-Cl-5-FC}_6\text{H}_3)$),^{7b} B5 ($\text{B}(p\text{-HC}_6\text{F}_4)_3$),^{7a} B6 ($\text{B}(\text{C}_6\text{F}_5)_3$),^{7a} and B7 ($\text{B}(\text{C}_6\text{F}_5)_2(\text{C}_6\text{Cl}_5)$).^{7a} Lewis acids B1, B2, and B3 yield amines, while B5, B6, and B7 yield imines. To

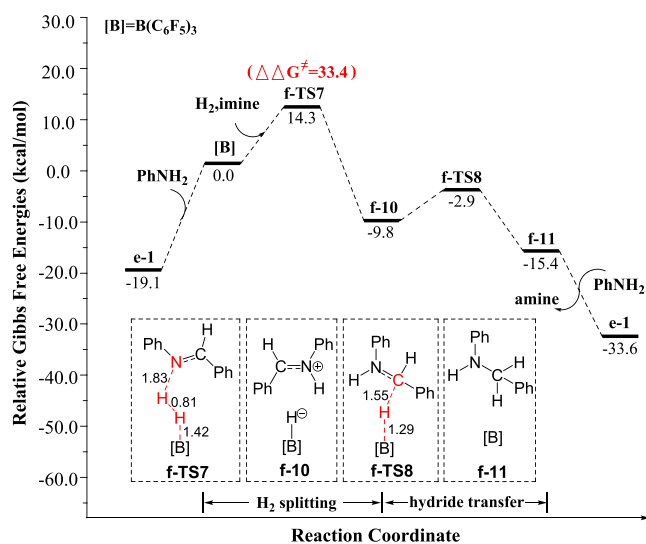


Figure 9. Free-energy profile of $\text{B}(\text{C}_6\text{F}_5)_3$ -catalyzed reduction of imine by dihydrogen. Optimized structures of the stationary points (key bond lengths are given in Å).

explore how the Lewis acid catalyst determines the selectivity of products, the natural charge on the boron atom and the hydride affinities of different catalysts are compared.

The values listed in Table 3 demonstrate that the charge on the boron atom in Lewis acid is linearly related to the relative energies of the Lewis adduct and the H_2 splitting transition state ($R^2 = 0.99$ and 0.97, respectively, as shown in Figure 10a). When the natural charge on the boron atom is large (e.g., B1, B2, and B3), the relative energy of the Lewis adduct is small, but that of the transition state is moderate. This results in a moderate free-energy barrier, which means that the amination reaction can occur under experimental conditions. However, when the natural charge on the boron atom is small (e.g., B5, B6, and B7), the energy of the H_2 splitting transition state is low, but the Lewis adduct is highly stable, resulting in a large free-energy barrier. Consequently, the cleavage of H_2 cannot easily occur. With correlation coefficients of 0.79 and 0.82, the relations between hydride affinity and Lewis adduct energy and H_2 splitting transition state are not linear. Therefore, the stability of the Lewis adduct and the efficiency of H_2 splitting are more influenced by the natural charge on the boron than by hydride affinity. Based on the data listed in Table 3, amines are produced when the natural charge on boron is larger than 1, but imines are produced when this charge is smaller than 1 (Figure 10b).

In addition, the product of reductive aniline and benzaldehyde amination by dihydrogen is imine when the Lewis acid is BPh_3 in experiments.^{7a} The natural charge on boron in BPh_3 is 0.93, indicating that the Lewis acid BPh_3 also follows the rule in Figure 10b. The free-energy barrier of H_2 splitting by BPh_3 and aniline is 28.9 kcal mol⁻¹, generating an ion pair. Then benzaldehyde is reduced by the ion pair, but the reaction needs to overcome a free-energy barrier of 31.0 kcal mol⁻¹. Thus, it is difficult for BPh_3 to produce amine following a path similar to pathway A, but produce imine following pathway B.

Based on the obtained results, two Lewis acids (B4, $\text{B}(2,6\text{-Cl}_2\text{C}_6\text{H}_3)(2,6\text{-Cl}_2\text{C}_6\text{F}_3)(3,5\text{-F}_2\text{C}_6\text{H}_3)$ and B8, $\text{B}(p\text{-ClC}_6\text{F}_4)_3$) were designed. The natural charges on boron atoms in the designed B4 and B8 catalysts are 1.08 and 0.89, respectively.

Table 3. Natural Charge on Boron Atom and Hydride Affinities of the Eight Lewis Acids^{7a,bab}

	B1 ^{7a}	B2 ^{7b}	B3 ^{7b}	B4 ^b	B5 ^{7a}	B6 ^{7a}	B7 ^{7a}	B8 ^b
Main product	Amine				Imine			
$e(B)$	1.00	1.05	1.12	1.08	0.90	0.89	0.98	0.89
Hydride affinity	72.1	63.7	63.1	66.7	76.1	78.2	75.1	80.3
G (adduct)	-10.4	-6.6	1.9	-1.7	-18.8	-19.1	-11.6	-20.2
$G(TS)$	17.8	22.0	27.2	20.3	14.0	12.5	18.4	15.2
$\Delta G(TS)$	28.2	28.6	27.2	22.0	32.8	31.6	30.0	35.4

^aRelative energies of the adducts and transition states implicated in the reductive aniline and benzaldehyde amination reaction catalyzed by different Lewis acids (units of kcal mol⁻¹). ^bDesigned Lewis acid.

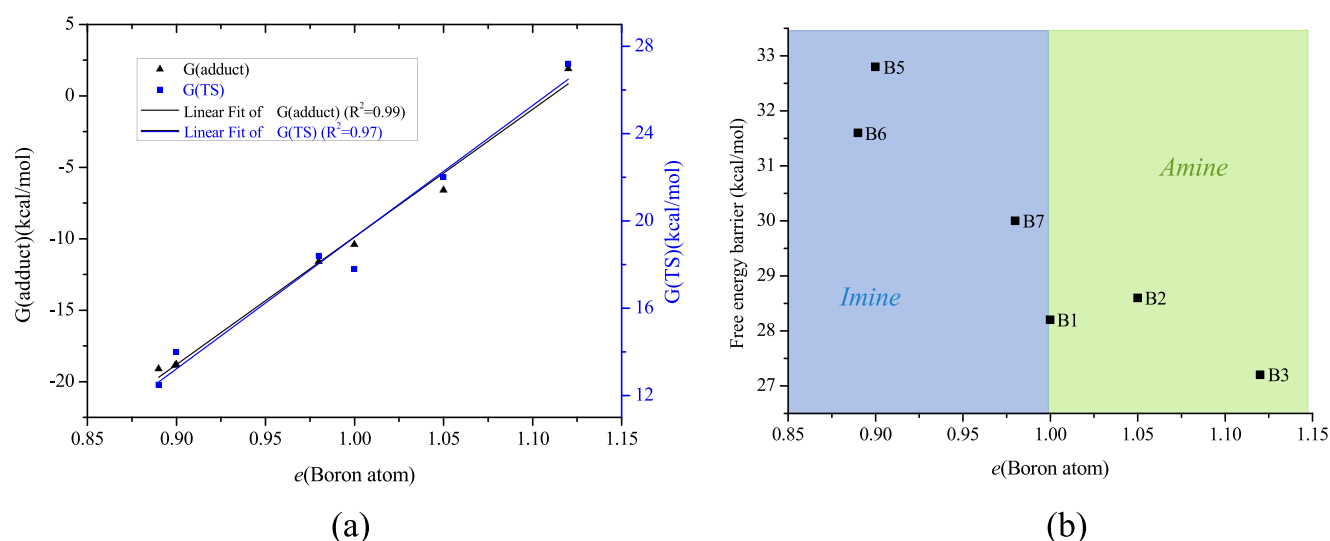


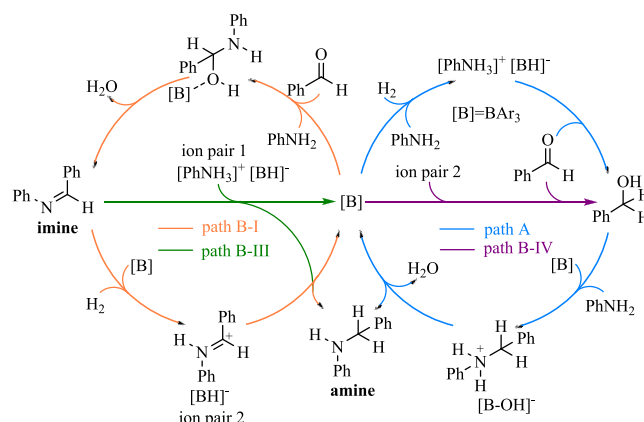
Figure 10. Relationship between the charge of the boron atom in the Lewis acid and the relative energies of the adduct and transition states.

Based on the above discussions, the B4-catalyzed amination of aniline and benzaldehyde by dihydrogen will yield an amine, while the B8-catalyzed reaction gives imine. Indeed, the free-energy barriers of H₂ splitting in the two reactions (B4- and B8-catalyzed) are 22.0 and 35.4 kcal mol⁻¹, respectively. Obviously, the results confirm that product selectivity can be predicted based on the natural charge on the boron atom in the Lewis acid.

3. CONCLUSIONS

In summary, this study uses DFT calculations to elucidate the detailed mechanism of borane-catalyzed reductive amination of aldehyde and aniline by the H₂ reducing agent. The results show that different borane catalysts give different products. When borane B(2,6-Cl₂C₆H₃)(*p*-HC₆F₄)₂ is used, the desired amine product is generated via four possible reaction pathways (paths A, B-I, B-III, and B-IV, summarized in Scheme 4). Paths A and B-IV involve the hydrogenation of benzaldehyde to form benzylic alcohol by different ion pairs (ion pairs 1 and 2; Scheme 4) followed by Lewis acid/base-promoted amine–alcohol condensation. Meanwhile, paths B-I and B-III involve an imine intermediate that undergoes hydrogenation by different ion pairs 1 and 2. The B(C₆F₅)₃-catalyzed N-

Scheme 4. Summary of the Possible Pathways of Borane-Catalyzed Reductive Amination of Ketones or Aldehydes with Anilines Using H₂ as the Reducing Agent



alkylation of amine and benzylic alcohol also proceeds via pathway A. The favorable pathway is dictated by the basicity of the Lewis base.

The product of the $B(C_6F_5)_3$ -catalyzed amination of aldehyde and aniline by H_2 is an imine. This is mainly due to the high stability of the adduct formed by coordination of $B(C_6F_5)_3$ and aniline, which increases the reaction barrier of imine hydrogenation. Considering that the charge on the boron atom in the Lewis acid is linearly related to the relative energies of the Lewis adduct and H_2 splitting transition state, the nature of the obtained product depends on this charge. Our calculations reveal that when the natural charge on the boron atom is larger than 1, the reaction gives amine, and when it is less than 1, the reaction gives imine. Therefore, the product of reductive aniline and benzaldehyde amination by H_2 can be controlled by adjusting the natural charge on the boron atom in the Lewis acid.

4. COMPUTATIONAL DETAILS

All calculations were performed using the Gaussian16 software package.¹⁴ The geometries and harmonic frequencies of all minima and transition states were optimized and calculated at the M06-2X/6-311G** level of theory.^{15,16} The calculated frequencies were used for thermal and entropic corrections at 298.15 K and 1 atm. The calculations were conducted in THF solvent (consistent with the experiment) using the self-consistent reaction field method and the IEFPCM solvation model.¹⁷ The important transition states were confirmed by IRC analysis.¹⁸ To obtain more accurate energies, the single-point energy calculations of the minimum energy conformers were conducted at the M06-2X/6-311++G** level of theory. Considering that the correction approach used herein is based on the ideal gas phase model, the contribution of entropy to free energy is expected to be overestimated. To account for such overestimation, a correction factor of -2.6 (or 2.6) kcal mol⁻¹ was added to all of the calculated free energies based on the “the theory of free volume.”¹⁹ Natural bond orbital analyses were performed at the M06-2X/6-311G** level to allocate partial atomic charges,²⁰ and IBO analyses were performed to study the electronic structure changes along the reaction pathway.²¹ The CYLview visualization program was used to display the 3D-optimized structures.²²

■ ASSOCIATED CONTENT

SI Supporting Information

The Supporting Information is available free of charge at <https://pubs.acs.org/doi/10.1021/acs.joc.1c02491>.

The optimized structures of all of the species in our studied reaction pathways, corrected free energies, imaginary frequency, and Cartesian coordinates (PDF)

■ AUTHOR INFORMATION

Corresponding Authors

Jiyang Zhao – School of Environmental Science, Nanjing Xiaozhuang University, Nanjing, Jiangsu 211171, China;
orcid.org/0000-0003-2397-4054; Email: jyzhao1981@163.com

Pan Du – School of Life Science and Chemistry, Jiangsu Second Normal University, Nanjing, Jiangsu 210013, China;
Email: shawwww@126.com

Authors

Shaoshan Liu – School of Environmental Science, Nanjing Xiaozhuang University, Nanjing, Jiangsu 211171, China

Shanshan Liu – School of Environmental Science, Nanjing Xiaozhuang University, Nanjing, Jiangsu 211171, China
Wenwen Ding – School of Environmental Science, Nanjing Xiaozhuang University, Nanjing, Jiangsu 211171, China
Sijia Liu – School of Environmental Science, Nanjing Xiaozhuang University, Nanjing, Jiangsu 211171, China
Yao Chen – School of Life Science and Chemistry, Jiangsu Second Normal University, Nanjing, Jiangsu 210013, China

Complete contact information is available at:
<https://pubs.acs.org/doi/10.1021/acs.joc.1c02491>

Author Contributions

[§]J.Z. and S.L. contributed equally.

Notes

The authors declare no competing financial interest.

■ ACKNOWLEDGMENTS

This work was supported by the Natural Science Foundation of the Jiangsu Higher Education Institutions of China (grant no. 18KJB150010 and 19KJB150034) and Foundation of Nanjing Xiaozhuang University (2018NXY24).

■ REFERENCES

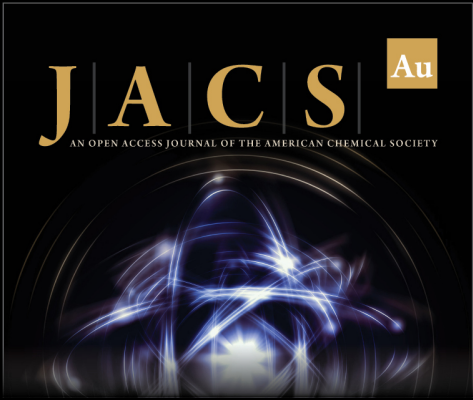
- (1) (a) Corey, E. J.; Czakó, B.; Kürti, L. *Molecules and Medicine*; WileyVCH: Weinheim, 2007. (b) Nicolou, K. C.; Montagnon, T. *Molecules That Changed the World*; Wiley-VCH: Weinheim, 2008.
- (2) (a) Lawrence, S. A. *Amines: Synthesis, Properties and Applications*; Cambridge University Press, 2004. (b) Salvatore, R. N.; Yoon, C. H.; Jung, K. W. Synthesis of secondary amines. *Tetrahedron* **2001**, *57*, 7785–7811. (c) Nugent, T. C.; el-Shazly, M. Chiral Amine Synthesis—Recent Developments and Trends for Enamide Reduction, Reductive Amination, and Imine Reduction. *Adv. Synth. Catal.* **2010**, *352*, 753–819. (d) Chusov, D.; List, B. Reductive Amination without an External Hydrogen Source. *Angew. Chem., Int. Ed.* **2014**, *53*, 5199–5201. (e) Fu, M.-C.; Shang, R.; Cheng, W.-M.; Fu, Y. Boron-Catalyzed N-Alkylation of Amines using Carboxylic Acids. *Angew. Chem., Int. Ed.* **2015**, *54*, 9042–9046. (f) Renaud, J.-L.; Gaillard, S. Recent Advances in Iron- and Cobalt-Complex-Catalyzed Tandem/Consecutive Processes Involving Hydrogenation. *Synthesis* **2016**, *48*, 3659–3683. (g) Andrews, K. G.; Summers, D. M.; Donnelly, L. J.; Denton, R. M. Catalytic reductive N-alkylation of amines using carboxylic acids. *Chem. Commun.* **2016**, *52*, 1855–1858. (h) Faisca Phillips, A. M.; Pombeiro, A. J. L. Recent advances in organocatalytic enantioselective transfer hydrogenation. *Org. Biomol. Chem.* **2017**, *15*, 2307–2340. (i) Sharma, M.; Mangas-Sanchez, J.; Turner, N. J.; Grogan, G. NAD(P)H-Dependent Dehydrogenases for the Asymmetric Reductive Amination of Ketones: Structure, Mechanism, Evolution and Application. *Adv. Synth. Catal.* **2017**, *359*, 2011–2025.
- (3) (a) Constable, D. J. C.; Dunn, P. J.; Hayler, J. D.; Humphrey, G. R.; Leazer, J. J. L.; Linderman, R. J.; Lorenz, K.; Manley, J.; Pearlman, B. A.; Wells, A.; Zaks, A.; Zhang, T. Y. Key green chemistry research areas—a perspective from pharmaceutical manufacturers. *Green Chem.* **2007**, *9*, 411–420. (b) Guru, M. M.; Thorve, P. R.; Maji, B. Boron-Catalyzed N-Alkylation of Arylamines and Arylamides with Benzylic Alcohols. *J. Org. Chem.* **2020**, *85*, 806–819. (c) Meng, S.-S.; Tang, X.; Luo, X.; Wu, R.; Zhao, J.-L.; Chan, A. S. C. Borane-Catalyzed Chemoselectivity-Controllable N-Alkylation and ortho C-Alkylation of Unprotected Arylamines Using Benzylic Alcohols. *ACS Catal.* **2019**, *9*, 8397–8403. (d) Nori, V.; Dasgupta, A.; Babaahmadi, R.; Carbone, A.; Ariafard, A.; Melen, R. L. Triarylborane catalysed N-alkylation of amines with aryl esters. *Catal. Sci. Technol.* **2020**, *10*, 7523–7530.
- (4) (a) Welch, G. C.; Juan, R. R. S.; Masuda, J. D.; Stephan, D. W. Reversible, Metal-Free Hydrogen Activation. *Science* **2006**, *314*, 1124–1126. (b) Jupp, A. R.; Stephan, D. W. Review Special Issue: Big Questions In Chemistry. *Trends Chem.* **2019**, *1*, 35–48.

- (c) Hoshimoto, Y.; Ogoshi, S. Triarylborane-Catalyzed Reductive N-Alkylation of Amines: A Perspective. *ACS Catal.* **2019**, *9*, 5439–5444.
- (d) Murugesan, K.; Senthamarai, T.; Chandrashekar, V. G.; Natte, K.; Kamer, P. C. J.; Beller, M.; Jagadeesh, R. V. Catalytic reductive aminations using molecular hydrogen for synthesis of different kinds of amines. *Chem. Soc. Rev.* **2020**, *49*, 6273–6328.
- (5) (a) Fasano, V.; Radcliffe, J. E.; Ingleson, M. J. $B(C_6F_5)_3$ -Catalyzed Reductive Amination using Hydrosilanes. *ACS Catal.* **2016**, *6*, 1793–1798. (b) Kim, E.; Park, S.; Chang, S. Silylative Reductive Amination of α,β -Unsaturated Aldehydes: A Convenient Synthetic Route to β -Silylated Secondary Amines. *Chem.-Eur. J.* **2018**, *24*, 5765–5769.
- (6) Pan, Z.; Shen, L.; Song, D.; Xie, Z.; Ling, F.; Zhong, W. $B(C_6F_5)_3$ -Catalyzed Asymmetric Reductive Amination of Ketones with Ammonia Borane. *J. Org. Chem.* **2018**, *83*, 11502–11509.
- (7) (a) Hoshimoto, Y.; Kinoshita, T.; Hazra, S.; Ohashi, M.; Ogoshi, S. Main-Group-Catalyzed Reductive Alkylation of Multiply Substituted Amines with Aldehydes Using H_2 . *J. Am. Chem. Soc.* **2018**, *140*, 7292–7300. (b) Dorkó, É.; Szabó, M.; Kótai, B.; Pápai, I.; Domján, A.; Soós, T. Expanding the Boundaries of Water-Tolerant Frustrated Lewis Pair Hydrogenation: Enhanced Back Strain in the Lewis Acid Enables the Reductive Amination of Carbonyls. *Angew. Chem., Int. Ed.* **2017**, *56*, 9512–9516.
- (8) (a) Chen, H.; Yan, L.; Wei, H. Mechanism of Boron-Catalyzed N-Alkylation of Primary and Secondary Arylamines with Ketones Using Silanes under “Wet” Conditions. *Organometallics* **2018**, *37*, 3698–3707. (b) Sultana, M.; Paul, A.; Roy, L. Computational Investigation of the Mechanism of FLP Catalyzed H_2 Activation and Lewis Base Assisted Proton Transfer. *ChemistrySelect* **2020**, *5*, 13397–13406.
- (9) (a) Stephan, D. W.; Erker, G. Frustrated Lewis Pairs: Metal-free Hydrogen Activation and More. *Angew. Chem., Int. Ed.* **2010**, *49*, 46–76. (b) Lam, J.; Szkop, K. M.; Mosafari, E.; Stephan, D. W. FLP catalysis: main group hydrogenations of organic unsaturated substrates. *Chem. Soc. Rev.* **2019**, *48*, 3592–3612. (c) Stephan, D. W. The broadening reach of frustrated Lewis pair chemistry. *Science* **2016**, *354*, No. aaf7229. (d) Zhao, J.; Wang, G.; Li, S. Mechanistic insights into the full hydrogenation of 2,6-substituted pyridine catalyzed by the Lewis acid $C_6F_5(CH_2)_2B(C_6F_5)_2$. *Dalton Trans.* **2015**, *44*, 9200–9208.
- (10) (a) Heshmat, M.; Privalov, T. Water and a Borohydride/Hydronium Intermediate in the Borane-Catalyzed Hydrogenation of Carbonyl Compounds with H_2 in Wet Ether: A Computational Study. *J. Phys. Chem. B* **2018**, *122*, 8952–8962. (b) Gyömrő, Á.; Bakos, M.; Földes, T.; Pápai, I.; Domján, A.; Soós, T. Moisture-Tolerant Frustrated Lewis Pair Catalyst for Hydrogenation of Aldehydes and Ketones. *ACS Catal.* **2015**, *5*, 5366–5372. (c) Das, S.; Pati, S. K. On the Mechanism of Frustrated Lewis Pair Catalyzed Hydrogenation of Carbonyl Compounds. *Chem. – Eur. J.* **2017**, *23*, 1078–1085.
- (11) (a) Gumus, I.; Ruzgar, A.; Karatas, Y.; Gülcin, M. Highly efficient and selective one-pot tandem imine synthesis via amine-alcohol cross-coupling reaction catalysed by chromium-based MIL-101 supported Au nanoparticles. *Mol. Catal.* **2021**, *501*, No. 111363. (b) Zhang, Y.-Y.; Li, J.-X.; Ding, L.-L.; Liu, L.; Wang, S.-M.; Han, Z.-B. Palladium Nanoparticles Encapsulated in the MIL-101-Catalyzed One-Pot Reaction of Alcohol Oxidation and Aldimine Condensation. *Inorg. Chem.* **2018**, *57*, 13586–13593. (c) Wang, D.; Li, Z. Coupling MOF-based photocatalysis with Pd catalysis over Pd@MIL-100(Fe) for efficient N-alkylation of amines with alcohols under visible light. *J. Catal.* **2016**, *342*, 151–157. (d) Shiraiishi, Y.; Ikeda, M.; Tsukamoto, D.; Tanaka, S.; Hirai, T. One-pot synthesis of imines from alcohols and amines with TiO_2 loading Pt nanoparticles under UV irradiation. *Chem. Commun.* **2011**, *47*, 4811–4813. (e) Terrasson, V.; Marquie, S.; Georgy, M.; Campagne, J.-M.; Prim, D. Lewis Acid-Catalyzed Direct Amination of Benzhydryl Alcohols. *Adv. Synth. Catal.* **2006**, *348*, 2063–2067. (f) Zhao, Y.; Foo, S. W.; Saito, S. Iron/Amino Acid Catalyzed Direct N-Alkylation of Amines with Alcohols. *Angew. Chem., Int. Ed.* **2011**, *50*, 3006–3009. (g) Ohshima, T.; Ipposhi, J.; Nakahara, Y.; Shibuya, R.; Mashima, K. Aluminum Triflate as a Powerful Catalyst for Direct Amination of Alcohols, Including Electron-Withdrawing Group-Substituted Benzhydrols. *Adv. Synth. Catal.* **2012**, *354*, 2447–2452. (h) Nayal, O. S.; Thakur, M. S.; Kumar, M.; Kumar, N.; Maurya, S. K. Ligand-free Iron(II)-Catalyzed N-Alkylation of Hindered Secondary Arylamines with Non-activated Secondary and Primary Alcohols via a Carbocationic Pathway. *Adv. Synth. Catal.* **2018**, *360*, 730–737.
- (12) Du, P.; Zhao, J.; Liu, S.; Yue, Z. Insights into the nucleophilic substitution of pyridine at an unsaturated carbon center. *RSC Adv.* **2021**, *11*, 24238–24246.
- (13) (a) Rokob, T. A.; Hamza, A.; Stirling, A.; Pápai, I. On the Mechanism of $B(C_6F_5)_3$ -Catalyzed Direct Hydrogenation of Imines: Inherent and Thermally Induced Frustration. *J. Am. Chem. Soc.* **2009**, *131*, 2029–2036. (b) Hamza, A.; Sorochkina, K.; Kótai, B.; Chernichenko, K.; Berta, D.; Bolte, M.; Nieger, M.; Repo, T.; Pápai, I. Origin of Stereoselectivity in FLP-Catalyzed Asymmetric Hydrogenation of Imines. *ACS Catal.* **2020**, *10*, 14290–14301. (c) Hermeke, J.; Mewald, M.; Oestreich, M. Experimental Analysis of the Catalytic Cycle of the Borane-Promoted Imine Reduction with Hydrosilanes: Spectroscopic Detection of Unexpected Intermediates and a Refined Mechanism. *J. Am. Chem. Soc.* **2013**, *135*, 17537–17546.
- (14) M. J., Frisch; G. W., Trucks; H. B., Schlegel; G. E., Scuseria; M. A., Robb; J. R., Cheeseman; G., Scalmani; V., Barone; B., Mennucci; G. A., Petersson; H., Nakatsuji; M., Caricato; X., Li; H. P., Hratchian; A. F., Izmaylov; J., Bloino; G., Zheng; J. L., Sonnenberg; M., Hada; M., Ehara; K., Toyota; R., Fukuda; J., Hasegawa; M., Ishida; T., Nakajima; Y., Honda; O., Kitao; H., Nakai; T., Vreven; J. A., Montgomery, Jr.; J. E., Peralta; F., Ogliaro; M., Bearpark; J. J., Heyd; E., Brothers; K. N., Kudin; V. N., Staroverov; R., Kobayashi; J., Normand; K., Raghavachari; A., Rendell; J. C., Burant; S. S., Iyengar; J., Tomasi; M., Cossi; N., Rega; J. M., Millam; M., Klene; J. E., Knox; J. B., Cross; V., Bakken; C., Adamo; J., Jaramillo; R., Gomperts; R. E., Stratmann; O., Yazyev; A. J., Austin; R., Cammi; C., Pomelli; J. W., Ochterski; R. L., Martin; K., Morokuma; V. G., Zakrzewski; G. A., Voth; P., Salvador; J. J., Dannenberg; S., Dapprich; A. D., Daniels; O., Farkas; J. B., Foresman; J. V., Ortiz; J., Cioslowski; D. J., Fox, *Gaussian 16, Revision A.03*; Gaussian, Inc.: Wallingford, CT, 2016.
- (15) (a) Zhao, Y.; Truhlar, D.-G. Density Functionals with Broad Applicability in Chemistry. *Acc. Chem. Res.* **2008**, *41*, 157–167. (b) Zhao, Y.; Truhlar, D.-G. The M06 suite of density functionals for main group thermochemistry, thermochemical kinetics, noncovalent interactions, excited states, and transition elements: two new functionals and systematic testing of four M06-class functionals and 12 other functionals. *Theor. Chem. Acc.* **2008**, *120*, 215–241.
- (16) Krishnan, R.; Binkley, J.-S.; Seeger, R.; Pople, J.-A. Self-consistent molecular orbital methods. XX. A basis set for correlated wave functions. *J. Chem. Phys.* **1980**, *72*, 650–654.
- (17) Tomasi, J.; Mennucci, B.; Cammi, R. Quantum Mechanical Continuum Solvation Models. *Chem. Rev.* **2005**, *105*, 2999–3094.
- (18) (a) Fukui, K. The path of chemical reactions-the IRC approach. *Acc. Chem. Res.* **1981**, *14*, 363–368. (b) Hratchian, H.-P.; Schlegel, H.-B. *Theory and Applications of Computational Chemistry: The First 40 Years*, ed. Dykstra, C. E.; Elsevier: Amsterdam, 2005, 195–249.
- (19) (a) Benson, S.-W. *The Foundations of Chemical Kinetics*; McGraw-Hill: New York, 1960. (b) Liu, Q.; Lan, Y.; Liu, J.; Li, G.; Wu, Y.-D.; Lei, A. Revealing a Second Transmetalation Step in the Negishi Coupling and Its Competition with Reductive Elimination: Improvement in the Interpretation of the Mechanism of Biaryl Syntheses. *J. Am. Chem. Soc.* **2009**, *131*, 10201–10210. (c) Schoenebeck, F.; Houk, K.-N. Ligand-Controlled Regioselectivity in Palladium-Catalyzed Cross Coupling Reactions. *J. Am. Chem. Soc.* **2010**, *132*, 2496–2497. (d) Liu, B.; Gao, M.; Dang, L.; Zhao, H.; Marder, T.-B.; Lin, Z. DFT Studies on the Mechanisms of the Platinum-Catalyzed Diboration of Acyclic α,β -Unsaturated Carbonyl Compounds. *Organometallics* **2012**, *31*, 3410–3425.
- (20) (a) Wiberg, K.-B. Application of the pople-santry-segal CNDO method to the cyclopropylcarbanyl and cyclobutyl cation and to bicyclobutane. *Tetrahedron* **1968**, *24*, 1083–1096. (b) Reed, A.-E.;


Curtiss, L.-A.; Weinhold, F. Intermolecular interactions from a natural bond orbital, donor-acceptor viewpoint. *Chem. Rev.* **1988**, 88, 899–926. (c) Weinhold, F. Natural bond orbital analysis: A critical overview of relationships to alternative bonding perspectives. *J. Comput. Chem.* **2012**, 33, 2363–2379.


(21) Knizia, G.; Klein, J. E. M. N. Electron Flow in Reaction Mechanisms—Revealed from First Principles. *Angew. Chem., Int. Ed.* **2015**, 54, 5518–5522.


(22) Legault, C.-Y. *CYLVview, 1.0b*; Université de Sherbrooke, 2009, <http://www.cylvview.org>



JACS **Au**
AN OPEN ACCESS JOURNAL OF THE AMERICAN CHEMICAL SOCIETY

 Editor-in-Chief
Prof. Christopher W. Jones
Georgia Institute of Technology, USA

Open for Submissions 

pubs.acs.org/jacsau  **ACS Publications**
Most Trusted. Most Cited. Most Read.